

Assessing Meteorological Effects on Vertical Coordinates with a Total Station

Introduction

Geodetic measurements, crucial for precise monitoring, are often influenced by atmospheric conditions, a factor that is sometimes overlooked or underestimated. In this project, we explore how various meteorological factors impact slope distance measurements. By examining these relationships, we aim to better understand and counteract the atmospheric effects on geodetic practices. We also analyze the manufacturer's distance correction model, which considers several meteorological parameters [1]. This analysis will reveal the extent to which certain impacts can be reduced and what residual effects persist. Furthermore, we apply various atmospheric corrections and evaluate the use of either high-end or low-end meteorological sensors for different atmospheric parameters. This will help determine which simplifications are acceptable for meeting specific accuracy needs in geodetic applications.

Field measurements

The first step in conducting the measurements is the determination of the optimal placement for the instruments and also the selection of an appropriate time interval. Regrettably, we were unable to carry out the measurements ourselves due to the ongoing construction work on the roof. We would like to express our gratitude to Lorenz Schmid and Nathalie Ryter for providing us with the necessary data.

Project perimeter

Figure 1 displays the locations of the five points used for conducting the measurements. The red points, identified as 1012, 1013, and 1014, are on top of the HIL building at the Campus Hönggerberg, ETH Zurich. Point 1020 is located over a hundred meters away from the HIL building, whereas the new point 1060 is positioned at the football field.



Figure 1: Map shows location of new point in blue and known fixed points in red

Equipment

Two Leica TS60 total stations (COM28 and COM29) were used for conducting the measurements. Additionally, various meteorological measurement stations are available at various price points, as shown in Table 1. Meteo Huts are equipped with various types of sensors. TMP116 sensors measure temperature, SHT31 sensors monitor humidity and temperature, while BME280 sensors measure humidity, pressure, and temperature. Each Meteo Hut is equipped with these three types of sensors. Both Reinhardt Stations are equipped with sensors that measure various environmental factors, including air pressure, temperature, and humidity, with the MWS9-5 station offering more variety at a steeper price point.

Meteo Station	Prize
Reinhardt Station MWS9-5	High-Cost
Reinhardt Station DFT1MW	High-Cost
GSEG Meteo Hut Lab 19	Low-Cost
GSEG Meteo Hut Lab 20	Low-Cost
GSEG Meteo Hut Lab 22	Low-Cost
GSEG Meteo Hut Lab 24	Low-Cost
GSEG Meteo Hut Lab 26	Low-Cost

Table 1: Meteo stations used for the project.

Measurement setup

For the field measurements, the two total stations, COM28 and COM29, were positioned on the rooftop of the HIL building between the two fixed points 1013 and 1014, as illustrated in Figure 2. Furthermore, the Meteo Huts Lab19, Lab20, Lab22, and the Reinhardt Station MWS9-5 were deployed on the HIL building. Meanwhile, the stations Lab22, Lab24, and DFT1MW were stationed at point 1060.



Figure 2: Instrument setup used for conducting the measurements.

Calibration of meteorological sensors

Sensor measurements often exhibit systematic deviations from the ground truth values. Therefore, it is crucial to calibrate sensors before utilizing them in practical applications. By assessing the deviation from

the ground truth, a correction model can be applied to enhance the reliability of a sensor in a post-processing step. The project data includes a time series from a calibration process conducted in the institute's climate-controlled test chamber for each sensor. The calibration involved setting the chamber to specific temperatures within the range of 5° to 35° C and maintaining these levels for several hours before transitioning to the next temperature step. Furthermore, an accurate reference sensor was present throughout the process, serving as the ground truth value for the model calibration. Examples of such time series are visualized at the top of Figures 3, 4, and 5. In this chapter, we present the calibration model we estimated based on the measurements inside the climate-controlled test chamber.

Development of calibration model

By identifying a suitable calibration model, the deviation of a sensor's measurement from the reference value can be minimized. This deviation can be assessed using the Root Mean Squared Error (RMSE). In Figure 3, the top section displays the recorded air pressure by Meteo Hut Lab19 alongside measurements from the reference sensor. There is a systematic deviation between the two sensors. We explored various calibration approaches for meteorological sensors, including a constant offset, linear regression, polynomial regression, and random forest. Initially, we divided the available data into a training set (80%) and a test set (20%) to evaluate the performance of each model.

While all methods demonstrated a strong performance on non-overlapping data, we selected the vertical shift as our proposed model. Its application in the calibration of meteorological sensors is justified for several reasons. Firstly, the actual measurements were taken outside, where the ambient temperature is oftentimes lower than that within the calibration room. This discrepancy between the environments can lead to inaccuracies in sensor readings. Secondly, while non-linear or machine learning methods for calibration may offer greater accuracy, their predictions tend to be less robust when applied to data that extends beyond the range of the calibration set, known as extrapolation. For the high-cost Reinhardt stations, it remains unclear whether their measurement accuracy is lower than the measurements taken by the reference sensor used as the ground truth. By employing a less complex model, we avoid the risk of overfitting a potentially more accurate sensor to the reference.

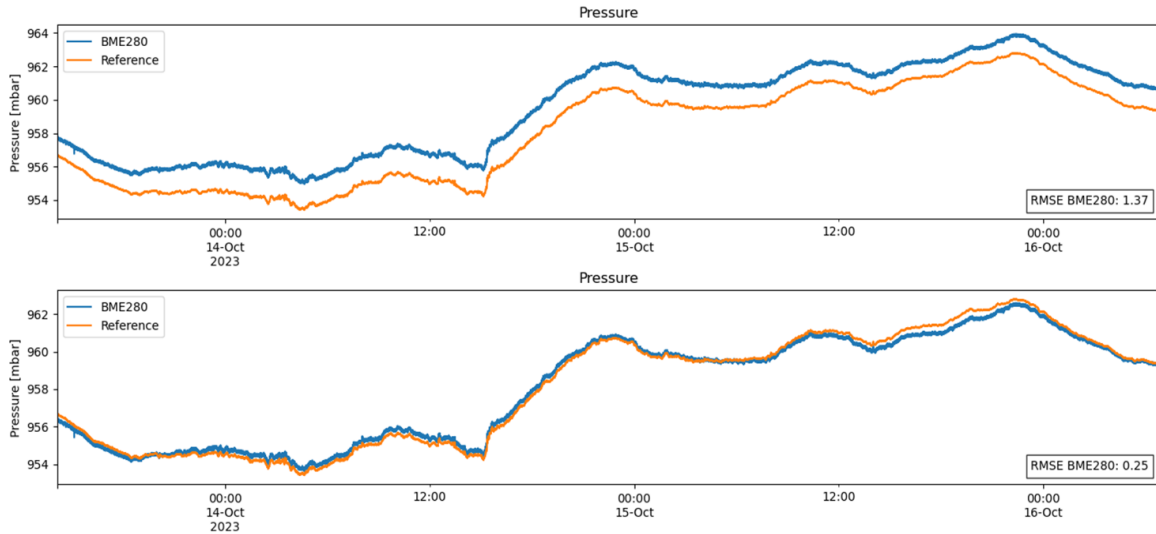


Figure 3: Time series of air pressure measured by Meteo Hut Lab19. The top plot illustrates the raw measurements, while the bottom plot displays the data after applying the suggested calibration model.

For some time series, we removed outliers to improve offset estimations, where the difference between two consecutive measurements is calculated and then compared to a certain threshold. As the time interval between two measurements is small, depending on the sensor this might be two seconds, a temperature change of 2 °C is highly unlikely and thus classified as an outlier. Figure 4 shows an example of this procedure.

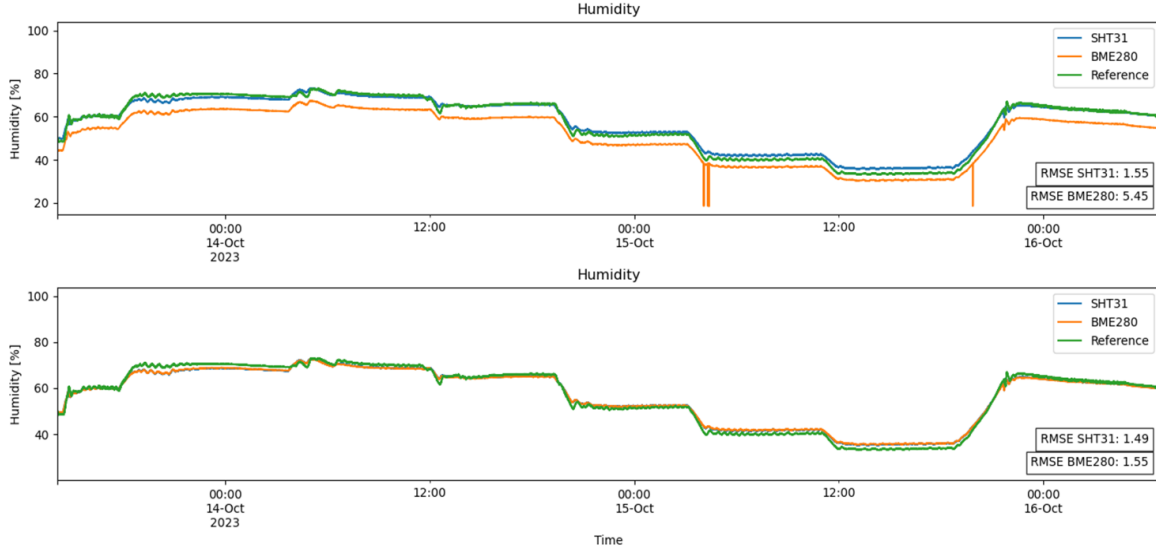


Figure 4: Time series of relative humidity measured by Meteo Hut Lab19. The top plot illustrates the raw measurements, while the bottom plot displays the data after applying the suggested calibration model.

The final model, which employs a vertical offset for each time series as seen in Table 2, delivered significant improvements compared to the uncalibrated case. Table 3 displays the Root Mean Squared Error (RMSE) of meteorological parameters measured by the Reinhardt stations and the best performing Meteo Hut at each location before and after calibration. Additionally, Figures 3 and 4 provide visual illustrations of the calibration model's effect, presenting raw data in the top plot and corrected data in the bottom plot.

Meteo Station	Meteorological parameters	Estimated offset
DFT1	Temperature [°C]	-1.768
	Pressure [mbar]	-4.575
	Humidity [%]	8.842
MSW95	Temperature [°C]	0.012
	Pressure [mbar]	1.054
	Humidity [%]	Used as reference sensor
Meteo Hut Lab19	Temperature [°C]	-0.528 (TMP116)
	Pressure [mbar]	-1.345 (BME280)
	Humidity [%]	-0.417 (SHT31)
Meteo Hut Lab24	Temperature [°C]	-0.553 (TMP116)
	Pressure [mbar]	-1.385 (BME280)
	Humidity [%]	0.142 (SHT31)

Table 2: Estimated offsets for the selected meteo stations.

Meteo Station	Meteorological parameters	RMSE before calibration	RMSE after calibration
DFT1	Temperature [°C]	1.88	0.63

	Pressure [mbar]	4.58	0.14
	Humidity [%]	9.09	2.11
MSW95	Temperature [°C]	0.23	0.23
	Pressure [mbar]	1.33	0.82
	Humidity [%]	Used as reference sensor	Used as reference sensor
Meteo Hut Lab19	Temperature [°C]	0.54 (TMP116)	0.12 (TMP116)
	Pressure [mbar]	1.37 (BME280)	0.25 (BME280)
	Humidity [%]	1.55 (SHT31)	1.49 (SHT31)
Meteo Hut Lab24	Temperature [°C]	0.56 (TMP116)	0.11 (TMP116)
	Pressure [mbar]	1.43 (BME280)	0.35 (BME280)
	Humidity [%]	1.50 (SHT31)	1.49 (SHT31)

Table 3: In-sample RMSE of meteorological parameters before and after calibration

The selection of optimal sensors for the subsequent distance corrections was based on the lowest root mean square error (RMSE) after adjusting for vertical offsets. The TMP116 sensor was chosen for temperature, the BME280 for pressure and the SHT31 for humidity.

Limitations of calibration model

While the vertical offset serves as a suitable model for calibration, there is still potential for improvements. Firstly, random fluctuations in the measurements by the reference sensor could be mitigated in a preprocessing step, allowing for an even more accurate calibration. Potential methods for this include low-pass filters, the moving average method, or even Kalman filtering. Secondly, the sensors tend to overshoot after fast meteorological changes, as illustrated in Figure 5. This overshooting introduces a small bias to the estimation of the vertical offset. By incorporating only measurements taken during episodes of constant temperature, the estimation of the offset parameter might be more accurate.

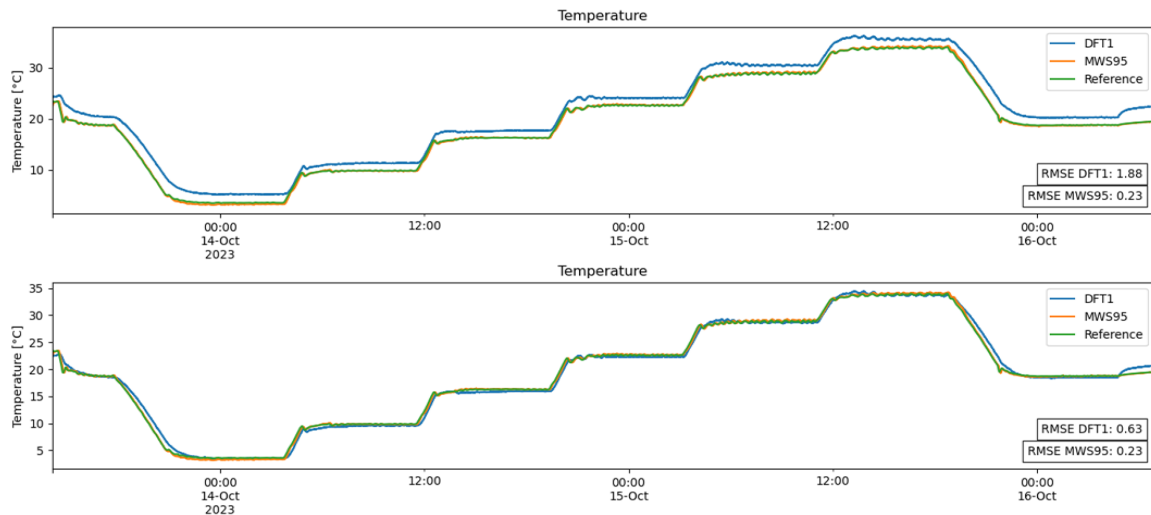


Figure 5: Time series of temperature measured by the Reinhardt stations. The top plot illustrates the raw measurements, while the bottom plot displays the data after applying the suggested calibration model.

Meteorological correction of measurements

The focus is set on determining how atmospheric conditions impact the data collected by the total station, specifically examining their effect on slope distance measurements. We mainly consider and evaluate the manufacturer's correction model in terms of sensitivity to meteorological parameters and the extent of correction it can provide. Additionally, we conduct our own analysis of the measurements in relation to meteorological data.

Before we conduct this analysis, outliers in the measurements are identified and removed using a similar approach to the one implemented in the calibration of the meteorological sensors, where we looked at the differences in consecutive measurements. The meteorological data is then corrected using the previously calculated offsets, before the atmospheric correction model is applied (see Figure 6) to determine the impact of meteorological parameters on the slope distance measurements. The calculated corrections are then added to the slope distance measurements using the formula in Figure 7, where the additive constant of the reflector was neglected.

$$\Delta D_1 = 286.338 - \left[\frac{0.29535 \cdot p}{(1 + \alpha \cdot t)} - \frac{4.126 \cdot 10^{-4} \cdot h}{(1 + \alpha \cdot t)} \cdot 10^x \right]$$

002419_002

ΔD_1 Atmospheric correction [ppm]

p Air pressure [mbar]

t Air temperature [$^{\circ}$ C]

h Relative humidity [%]

$\alpha = \frac{1}{273.15}$

x $(7.5 * t / (237.3 + t)) + 0.7857$

Figure 6: Atmospheric correction model for Leica TS60 [1].

$$\triangle = D_0 \cdot (1 + ppm \cdot 10^{-6}) + mm$$

TS_111

\triangle Displayed slope distance [m]
 D_0 Uncorrected distance [m]
ppm Atmospheric scale correction [mm/km]
mm Additive constant of the reflector [mm]

Figure 7: Computation of corrected slope distance [1].

Analysis of meteorological parameters

As a major part of the project, we analyze patterns and relationships in the measured data presented in this chapter. More specifically, we analyze the correlations of the meteorological measurements over time, the influence of the used meteorological sensors on the standard deviation of slope distance measurements, and other comparisons.

Meteorological measurements

Figure 8 shows the meteorological measurements of Lab24. Temperature and humidity are subject to rapid fluctuations, which can be attributed to the daily changes in weather. For instance, the temperature graph illustrates significant spikes and drops within a short timeframe, indicating quick responses to daily weather patterns. Conversely, atmospheric pressure demonstrates a gradual and steady trend, changing

slowly over time. This suggests that pressure is influenced more by larger-scale weather systems rather than the quick transitions seen in temperature and humidity.

Furthermore, a strong negative correlation exists between temperature and relative humidity. As temperature rises, humidity tends to decrease, and conversely, when temperature falls, humidity increases. This behavior aligns with the principles of thermodynamics, specifically reflecting the inverse relationship predicted by physical laws describing the interaction between temperature and humidity.

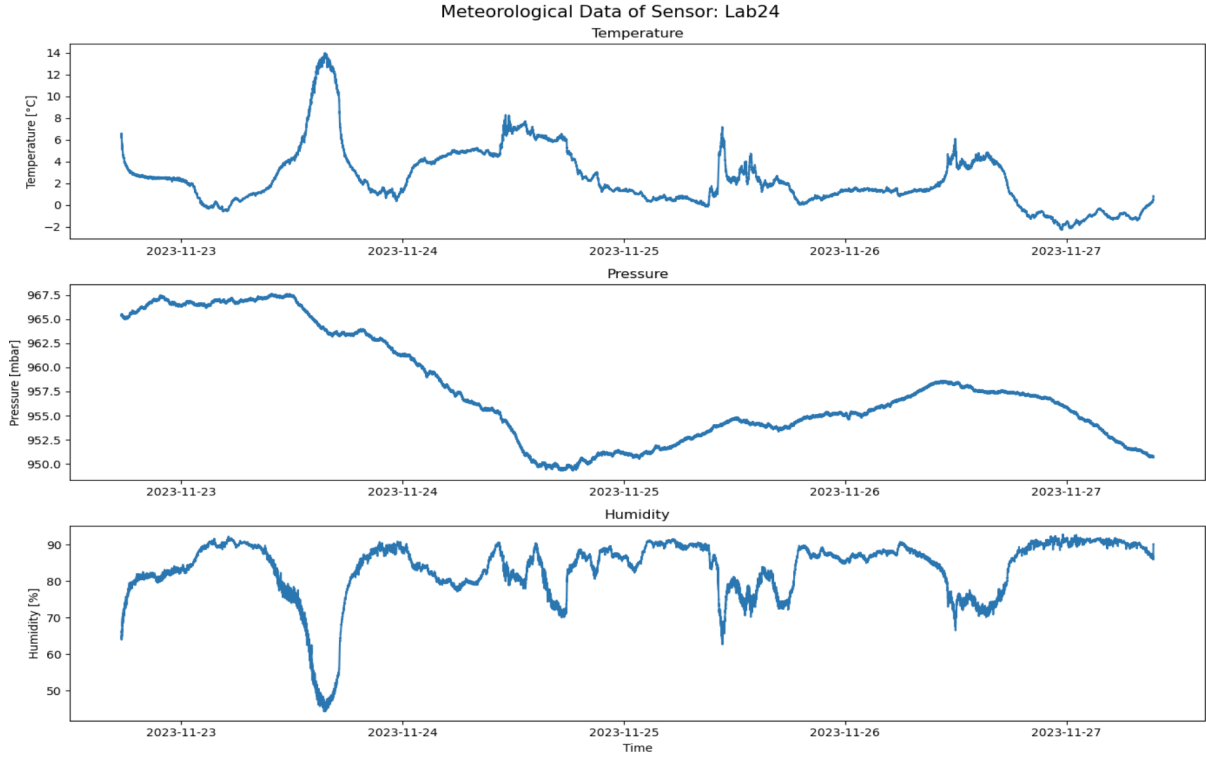


Figure 8: Meteorological measurements over time by Meteo Hut Lab24 placed at point 1060.

Best time for measuring

Figure 9 shows that during the night, the temperature remains mostly constant, leading to stable distance corrections. This stability simplifies the identification of outliers, as the corrections do not fluctuate wildly. The temperature during the day changes much faster. Such variability can introduce complexity in the data analysis and may affect the accuracy of the measurements. Thus, nighttime conditions appear to be more beneficial for precise measurements.

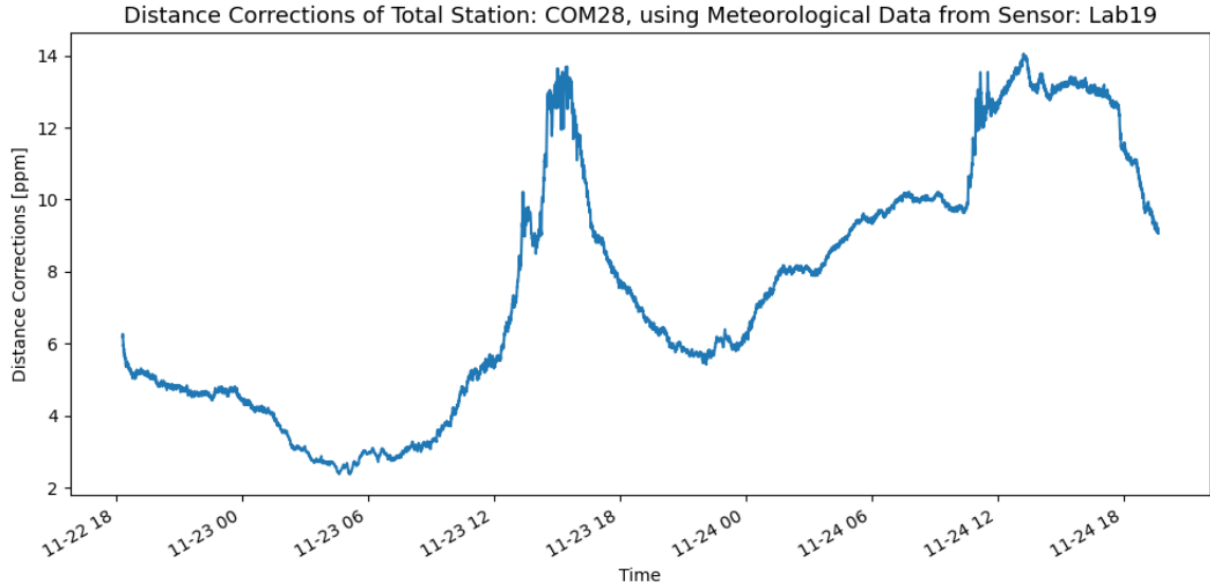


Figure 9: Distance corrections over time, calculated using meteorological data recorded by Meteo Hut Lab19.

Standard deviations of the measured distances

To assess the impact of individual sensors on distance measurements, we calculated the standard deviations of the slope distances. We corrected each distance measurement using meteorological data from a specific sensor. The results obtained in millimeters are presented in Tables 4 and 5. We assess the performance of four stations: MWS9-5, DFT1MV (high-cost sensors), LAB19 (near total station) and LAB24 (near target 1060).

Station Name	Std point 1014	Std point 1012	Std point 1013	Std point 1020	Std point 1060	Mean Std
MWS9-5	0.168	0.149	0.138	0.409	0.338	0.240
DFT1MV	0.167	0.151	0.138	0.453	0.323	0.246
LAB19	0.160	0.149	0.143	0.844	0.299	0.319
LAB24	0.178	0.147	0.137	1.097	0.421	0.396

Table 4: Standard deviation of slope distance measured by COM28 (unit: mm)

Station Name	Std point 1014	Std point 1012	Std point 1013	Std point 1020	Std point 1060	Mean Std
MWS9-5	0.373	0.225	0.288	0.313	0.212	0.282
DFT1MV	0.515	0.229	0.284	0.309	0.212	0.310
LAB19	0.822	0.314	0.211	0.230	0.197	0.355
LAB24	1.072	0.331	0.294	0.316	0.212	0.445

Table 5: Standard deviation of slope distance measured by COM29 (unit: mm)

Based on the results presented in Tables 4 and 5, we discovered some fascinating insights:

a. Magnitude of standard deviation

The magnitude of the effects of the meteorological conditions align with our expectations (mm/km). Most measured distances have a standard deviation in the same order of magnitude as reported of the instrument accuracy by Leica ($0.6\text{mm} \pm 1\text{ppm}$) [2].

b. Low-cost and high-cost sensors

The mean standard deviation of the high-cost Reinhardt stations (MWS9-5 and DFTIMV) and the low-cost Meteo Huts (Lab19 and Lab24) suggests that high-cost sensors allow for more accurate meteorological corrections; however, the difference in performance between high-cost and low-cost sensors is only marginal. For most applications, low-cost sensors should suffice as their corrected distances have standard deviations in the same order of magnitude as the high-cost versions. However, users requiring the highest precision should still consider the use of high-cost sensors, as they offer some benefits.

c. Meteorological station at the total station and target location

The sensors DFT1MV and Lab24 are positioned at point 1060, whereas the remaining sensors are situated on the roof of the HIL building. Upon comparing the standard deviations of the sensor readings from both locations, it is clear that the standard deviations of distances corrected with meteorological adjustments from the roof are lower.

d. Differences between the total stations

Not only do meteorological parameters impact the standard deviation of measurements, but the choice of instrument also plays a crucial role. The total station COM28 exhibits a mean standard deviation across all measurements (all points and sensors) of 0.300mm, whereas the total station COM29 displays a larger standard deviation of 0.348mm.

e. Differences between the measured slope distance

The measured points exhibit varying slope distances from the total stations. The farthest point is point 1060, with a slope distance of approximately 600m, followed by point 1020, with a distance of about 130m. The remaining points all have distances below 30 meters from both total stations. No significant patterns emerge by comparing the standard deviations among the points, indicating that longer distances do not consistently result in larger standard deviations.

Comparison between corrected and raw distances

Meteorological corrections are crucial for ensuring the required quality of measured distances. Figure 10 presents time series data for raw and corrected distances. The top two plots represent corrections using measurements from the best-performing Reinhardt station, while the bottom two plots are derived from Meteo Hut Lab24. Point 1060 is approximately 600m away, whereas point 1014 is within 30m of the total station COM28. The plots clearly illustrate that distance corrections increase with larger distances. While raw distances to point 1013 sometimes fall within the standard deviation of the corrected distances, there is no overlap between raw and corrected measurements for the more distant point 1060. These results align with the expectations based on the correction formula outlined in an earlier chapter.

Notably, the Meteo Hut Lab24 exhibits a significant systematic deviation lasting approximately two hours on November 23, as evident from the positive peak. The cause of this deviation remains unclear, but it is plausible that the used sensor may be faulty. This pattern is not observed in the corrected distance from the Reinhardt station.



Figure 10: Raw and corrected distance measurements over time.

Determination of height coordinate

While the project's time schedule did not allow for the computation of the height coordinates for the new point 1060, we nevertheless provide a short description of our approach: First, we would calculate the mean of distance measurements conducted during the night between 2 and 4 am, excluding outliers in a post-processing step. Next, we would apply meteorological corrections based on data from the best-performing Reinhardt station, MWS9-5, adjusted by our estimated offset. Afterwards, we need to determine the height of the total station by using the fixed points as reference. Once we have done that, we can use the following formula in Figure 11 (trigonometric height transfer) to estimate the height of the new point.

$$H_{Target} = H_{Instrument} + d * \sin(\text{zenith angle}) + \frac{(d * \cos(\text{zenith angle}))^2}{2 * R}$$

Figure 11: Formula for trigonometric height transfer.

Limitations and improvements

While our approach has resulted in distance measurements with low standard deviations, there is still room for further improvements. The meteorological correction model does not contain all variables, such as solar radiation during the day or atmospheric refraction. Additionally, it is insufficient to rely exclusively on distance measurements to determine height coordinates, as angles also play a crucial role. Specifically, considering meteorological influences could enhance the accuracy of zenith angles. Furthermore, it is important to note that the measurements would still exhibit a random component even if external influences were corrected perfectly, for instance, due to the persistence of instrumental errors arising from electronic components in the measurement device. The distance measurement could be further improved by using the additional constant for distance deviation caused by the reflector, as shown in Figure 7. Furthermore, to obtain more precise meteorological data for corrections, it would also be beneficial to establish additional meteorological stations between the total station and the target, ensuring comprehensive coverage along the line of sight.

Conclusion and take-home message

Our analysis has provided fascinating insights into the impact of meteorological parameters on distance measurements. We have also conducted a detailed examination of meteorological corrections, which proves crucial, particularly for longer slope distances. While high-cost sensors show slightly superior performance, suggesting an advantage in achieving slightly more precision, the minimal difference in the standard deviation of slope distance measurements implies that the use of low-cost sensors could still be justified for less critical applications or when budget constraints are a concern. In cases where multiple sensors with varying performance levels are available, it is advisable to prioritize the use of the best-performing sensors rather than averaging measurements from all sensors. Averaging could inadvertently introduce errors from poorly performing sensors, potentially compromising the accuracy of measurements from the higher-performing sensors. Additionally, our results indicate that distance measurements may benefit from being conducted at night rather than during the day.

Finally, conducting large-scale studies and extensive statistical testing would be necessary to assess the generalizability of our results and interpretations. Furthermore, it is important to acknowledge that sensors can be faulty, highlighting the ideal use of multiple sensors for measurements. The accuracy of reference sensors should also be carefully assessed, as assuming a ground truth sensor is not guaranteed, especially if the reference sensor is not significantly more accurate than the sensor under comparison.

References

- [1] Leica Geosystems AG. (n.d.). Leica MS60/TS60 User Manual.
- [2] Leica Geosystems AG. (n.d.). Leica Nova TS60 Total Station Datasheet. Leica Geosystems AG. https://leica-geosystems.com/-/media/files/leicageosystems/products/datasheets/leica_nova_ts60_ds.ashx?la=de-de&hash=2CCBBCF7639E1F6647DAA23A6D10EB87